Nanoscale Advances

ROYAL SOCIETY OF CHEMISTRY

PAPER

View Article Online
View Journal | View Issue



Cite this: *Nanoscale Adv.*, 2024, **6**, 985

# First-principles calculations of inorganic metallocene nanowires†

Yangqi Ji,[a] Haifeng Lv *[ab] and Xiaojun Wu *[ab]

Received 26th October 2023
Accepted 29th December 2023

DOI: 10.1039/d3na00926b

rsc.li/nanoscale-advances

Inspired by the recently synthesized inorganic metallocene derivatives $Fe(P_4)_2^{2-}$, we have identified four stable inorganic metallocene nanowires, $MP_4$ (M = Sc, Ti, Cr and Fe) in configurations of either regular quadrangular prism (Q-type) or anticube (A-type), and further investigated their magnetic and electronic characteristics utilizing the first-principles calculation. It shows that $CrP_4$ is a ferromagnetic metal, while other nanowires are semiconducting antiferromagnets with bandgaps of 0.44, 1.88, and 2.29 eV within the HSE06 level. It also shows that both $ScP_4$ and $TiP_4$ can be stabilized in the Q-type and A-type, corresponding to the antiferromagnetic and ferromagnetic ground states, respectively, indicating a configuration-dependent magnetism. The thermodynamic and lattice stabilities are confirmed by the *ab initio* molecular dynamics and phonon spectra. This study has unmasked the structural and physical properties of novel inorganic metallocene nanowires, and revealed their potential application in spintronics.



## Introduction

Since the milestone discovery of ferrocene,[1] the multidecker molecular complexes in the form of sandwich clusters and their infinitely extended nanowires have attracted great research interest due to the distinct structural, optical,[2,3] chemical,[4] electrical,[5] and magnetic properties,[6] rendering them potential candidates in catalysis,[7] electronics and spintronics.[8–12] Especially, the tunable coordination mode between the central metal and organic molecules accompanied by diverse charge transfer and crystal field splitting can lead to unpaired d electrons and form intriguing magnetic ordering phenomena.[13–15] For instance, the organometallic complexes composed of vanadium and benzene, $V_n(Bz)_m$ (Bz = $C_6H_6$), were confirmed to be molecular magnets and the magnetic moments of the complexes increase with the central metal atoms.[16,17] Then, theoretical study revealed that the one-dimensional $[V(Bz)]_\infty$ and $[Mn(Bz)]_\infty$ are quasi- or half-metallic.[18] Also, $(VCp)_\infty$ (Cp = $C_5H_5$), $(VBzVCp)_\infty$, and $(V_2Ant)_\infty$ wires (Ant = anthracene) are ferromagnetic half-metals.[19] Based on pentalene (Pn = $C_8H_6$), double metallocene nanowires were predicted, in which the $PnMn_2$ nanowire exhibits ferromagnetic behavior.[20] Among the homo-bimetallic naphthalene (Np=$C_{10}H_8$), namely $NpTM_2$, (TM = V, Mn, Ti, Nb) nanowires, $NpMn_2$ is ferromagnetic, $NpTi_2$ and $NpNb_2$ are antiferromagnetic, and $NpV_2$ exhibits carrier-tunable magnetic ordering.[21] Then, the hetero-bimetallic naphthalene nanowires, $[Np_2V_2Cr_2]_\infty$, $[Np_2V_2Mn_2]_\infty$, and $[Np_2V_2Fe_2]_\infty$ are shown as half-metals, while $[Np_2V_2Cr_2]_\infty$ is quasi-half-metallic,[22] and the $V_{n-1}Np_n$ nanowire also exhibits carrier-tunable magnetic ordering.[23] Theoretical studies also demonstrated that the sandwiched $Eu_nCOT_{n+1}$ (Eu = europium, COT = $C_8H_8$, $n$ = 1–4) clusters are molecular magnets.[24] By using the chemical functionalization, the multiferroic organometallic molecular nanowires were predicted.[25] A recent study showed that ferromagnetic half-metallicity can be realized in metal trihydride molecular nanowires.[15] As a result, exploring novel metallocene-analogue molecular clusters and nanowires with magnetism is highly desirable due to their high potential application as one-dimensional spintronics.

To enrich the family of multidecker sandwich complexes, great efforts have been made to explore molecules similar to ferrocene and it is assumed that a heteroelement derivative can be obtained by the isolobal replacement of CH with group 15 phosphorus, which may possess distinct properties with various bond types and coordination environment.[26] Despite the high stability of $Fe(\eta^5\text{-}P_5)_2$ confirmed by the theoretical calculation,[27] experimental realization has not been achieved, and only a molecular complex $Ti(\eta^5\text{-}P_5)_2$ was reported to be synthesized so far.[28] Cyclo-$P_4$, which can accommodate two electrons, is believed to be more useful in contrast to the monoanionic cyclo-$P_5$.[29] Very recently, Wang *et al.* has synthesized a ferrocene derivative $[Fe(P_4)_2]^{2-}$ by using Zintl ions as precursors,[30] which may serve as the building block for the inorganic metallocene complexes.

Enlighted by the recently synthesized $Fe(P_4)_2^{2-}$, inorganic metallocene nanowires, $MP_4$ (M = Sc, Ti, Cr and Fe) are reported

[a]*School of Chemistry and Materials Science, CAS Key Laboratory of Materials for Energy Conversion, CAS Center for Excellence in Nanoscience, University of Science and Technology of China, Hefei, Anhui 230026, China*

[b]*Key Laboratory of Precision and Intelligent Chemistry, University of Science and Technology of China, Hefei, Anhui 230026, China. E-mail: xjwu@ustc.edu.cn*

† Electronic supplementary information (ESI) available: Phonon spectrum calculations; AIMD results; density of states; energy differences between the A-type and Q-type nanowires; magnetic anisotropy energy for the nanowires. See DOI: https://doi.org/10.1039/d3na00926b

and the structural, electrical, and magnetic characteristics are investigated within the first-principles calculation. Our results show that $ScP_4$, $TiP_4$, $CrP_4$ and $FeP_4$ can form stable one-dimensional nanowires in either regular quadrangular prism (Q-type) or anticube (A-type) configurations. Among them, $ScP_4$, $TiP_4$ and $FeP_4$ nanowires have antiferromagnetic (AFM) ground state and $CrP_4$ nanowires are ferromagnetic (FM). AIMD simulation and phonon spectrum calculations have confirmed their thermodynamic and lattice stabilities.

## Methods

First-principles calculations were performed by using the Perdew–Burke–Ernzerhof (PBE) functional and Projector Augmented Wave (PAW) potential within the Vienna *ab initio* simulation (VASP) package.[31–35] A cut-off energy of 400 eV was adopted, and the atomic positions and lattice constant along the extended direction were relaxed until the force and energy were smaller than 0.01 eV $Å^{-1}$ and $1 \times 10^{-5}$ eV. A $\Gamma$-centered $1 \times 1 \times 8$ $k$-points was used. According to the previous research,[36,37] a Hubbard $U_{eff}$ value of 3 eV was adopted to account for the strong correlation effect. To obtain a more accurate electronic structure, the Heyd–Scuseria–Ernzerhof hybrid functional (HSE06) was adopted.[38] One-dimensional chains were chosen to extend along the $c$-axis, while a certain vacuum layer thickness (around 10 Å) is added in the other directions of the unit cell to avoid repetitive disturbances of the force field under the periodic boundary conditions. Considering the van der Waals (vdW) interactions, the Grimme DFT-D3 correction was utilized.[39] Additionally, *ab initio* molecular dynamics (AIMD) simulations were executed with the supercell of $1 \times 1 \times 4$ and the total time was 5 ps with each step of 1 fs, using the *NVT* ensemble. The phonon spectra were calculated with density-functional-perturbation theory (DFPT) using PHONOPY.[40] The post-processing calculations for the relevant calculations were performed using the VESTA software[41] and VASPKIT code.[42]

## Results and discussion

According to Fig. 1(a), the $MP_4$ molecular complex is composed of one transition metal atom sandwiched between two square cyclo-$P_4$ rings, owning to the $C_{4v}$ symmetry and forming an $\eta^4$ : $\eta^4$ coordination pattern. The $P_4$ rings can arrange into two configurations, namely, regular quadrangular prism (Q-type) (Fig. 1(b)) or anticube (A-type) (Fig. 1(c)). Hence, two types of $MP_4$ nanowires are considered, as shown in Fig. 1(d) and (e), respectively. Then, the geometrical configurations of $MP_4$ nanowires (M = Sc to Ni) in Q-type and A-type are relaxed and it shows that $ScP_4$, $CrP_4$, and $FeP_4$ are energetically more stable in the Q-type and $TiP_4$ is energetically more stable in the A-type, as displayed in Table S1.† Cu and Zn are excluded due to their absence of metallocene forms. The lattice stability of the energetically stable $MP_4$ is identified according to their phonon spectra. As displayed in Fig. S1,† imaginary frequencies are absent for the $ScP_4$, $CrP_4$, and $FeP_4$, and a small imaginary frequency in $TiP_4$ nanowires is partly attributed to the flat potential energy surface at its ground state. Hence, the calculations below are based on the $ScP_4$, $TiP_4$, $CrP_4$ and $FeP_4$ nanowires.

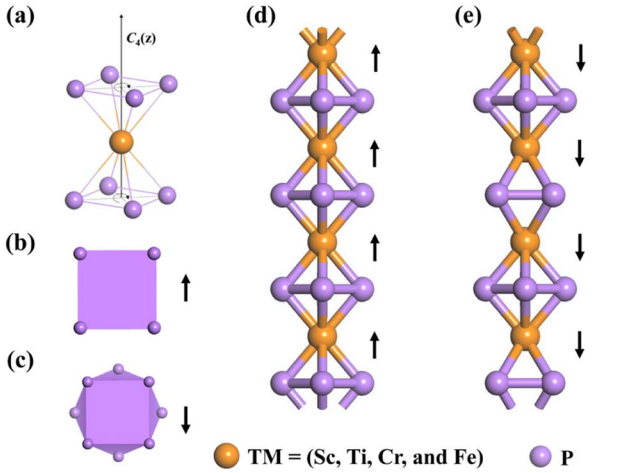


Fig. 1 Models of (a) $MP_4$ molecular complex, (b) regular quadrangular prism (Q-type) ligand field, (c) anticube (A-type) ligand field, (d) Q-type $MP_4$ nanowire, and (e) A-type $MP_4$ nanowire. The "up" and "down" arrows indicate the different stacking models of cyclo-$P_4$ rings.

As demonstrated in Table 1, the M–P distances exhibit a range of 2.46 to 2.70 Å, descending from Sc to Fe, and the P–P distances among adjacent P atoms vary from 2.24 to 2.28 Å, indicating the elongated P–P distance compared to black phosphorus (2.18 Å).[43] To further determine their stability, we calculated the averaged formation energy per unit cell, which is described as below, in which $E_{NW}[MP_4]$, $E[M]$, and $E[P_4]$ are the energies of the nanowire, single metal atom, and cyclo-$P_4$ ring, respectively.

$$E_f[MP_4] = E_{NW}[MP_4] - E[M] - E[P_4]$$

The calculated formation energies vary from −5.79 to −8.00 eV, in which the negative formation energies indicate that the formation of $MP_4$ nanowires from the $P_4$ ring and metal atom is exothermic, and $ScP_4$ nanowire has the largest formation energy. These values are larger or comparable to those for other organic multidecker nanowires, including transition

Table 1 Metal–phosphorus bond distance ($d_{MP}$, Å), phosphorus–phosphorus bond distance ($d_{PP}$, Å), averaged formation energy per unit cell ($E_f$, eV), transferred charge from the metal to phosphorus ($C$, e), and atomic magnetic moment ($M$, μB) on each metal atom, ground state (GS, in which S and M denote the semiconductor and metal), and energy difference ($\Delta E = E(FM) - E(AFM)$, eV) between ferromagnetic (FM) and antiferromagnetic (AFM) states per unit cell

| | $ScP_4$ | $TiP_4$ | $CrP_4$ | $FeP_4$ |
|---|---|---|---|---|
| $d_{MP}$ | 2.70 | 2.55 | 2.52 | 2.46 |
| $d_{PP}$ | 2.26 | 2.28 | 2.24 | 2.24 |
| $E_f$ | −8.00 | −7.99 | −5.79 | −6.43 |
| $C$ | 1.67 | 1.55 | 1.01 | 0.76 |
| $M$ | 0.16 | 0.80 | 3.31 | 3.21 |
| GS | AFM S | AFM S | FM M | AFM S |
| $\Delta E$ | 0.02 | 0.68 | −0.58 | 0.66 |

metal benzene nanowires (−1.71 to −5.33 eV) or metallocene nanowires.[18,44]

In addition, we also examined the thermodynamic stability of the $MP_4$ nanowires by conducting the *ab initio* molecular dynamics (AIMD) simulation at temperatures increasing up to 700 K. The evolution of total energy and magnetic moments along with time, and the last snapshots for the AIMD simulations are shown in Fig. S4.† It can be observed that the structural motif A-type $TiP_4$ nanowires can be maintained at 300 K. $CrP_4$ nanowires are able to maintain their structure at 400 K, $FeP_4$ at 500 K, and for $ScP_4$, the temperature can reach up to 700 K. The difference in thermodynamic stability can be elucidated by the energy difference between the A-type and the Q-type structures in the same magnetic ground state per unit cell, as shown in Table S1.† The energy difference between the Q-type and A-type $CrP_4$ nanowires in the FM state is the smallest (0.196 eV), and $ScP_4$ has the largest energy difference (0.759 eV), leading to different thermodynamic stabilities. Meanwhile, the poor thermodynamic stability of $TiP_4$ is partly attributed to the low oxidation state of central Ti.

Next, the magnetic ground states of the $MP_4$ nanowires are confirmed and three magnetic states are considered, ferromagnetic (FM), antiferromagnetic (AFM) states, and nonmagnetic states (NM). The $ScP_4$, $TiP_4$ and $FeP_4$ nanowires are identified to be antiferromagnetic, in which the energy differences are 0.02 eV, 0.68 eV and 0.66 eV between the FM and AFM states. Particularly, the $CrP_4$ nanowires are ferromagnetic in their ground state, which is 0.58 eV energetically lower than the AFM state. The atomic magnetic moments of Sc, Ti, Cr, and Fe atoms are 0.16, 0.80, 3.31, and 3.21 μB, respectively. We have provided the element-resolved density of states and the spatial distribution of CBM/VBM decomposed charge density in the real space for the three semiconducting nanowires at the same isosurface level in Fig. S5 and S9.† It shows that for $ScP_4$ (Fig. S9(a and b)†) the VBM and CBM are contributed by $d_{xy}$/$d_{x^2-y^2}$, for $TiP_4$ (Fig. S9(c and d)†) the VBM and CBM are contributed by $d_{xy}$/$d_{x^2-y^2}$ and $d_{z^2}$, respectively, for $FeP_4$ (Fig. S9(e and f)†) the VBM and CBM are contributed by $d_{xz}$/$d_{yz}$ and $d_{z^2}$, respectively, which is well-accorded with the calculated electronic structures in Fig. 2 and S6.†

Then, the band structures of the $MP_4$ nanowires are illustrated in Fig. 2. $ScP_4$ and $FeP_4$ nanowires have direct band gaps with bandgaps of 0.44 eV and 2.29 eV, and the $TiP_4$ nanowires have an indirect bandgap with bandgaps of 1.88 eV at the HSE06 level, respectively. Meanwhile, $CrP_4$ nanowires are metallic.

Next, we have tried to understand the origin of magnetism of the $MP_4$ nanowires. In a regular quadrangular prism crystal field, five 3d orbitals of metal atoms are readily split into a doubly degenerate band e ($d_{xz}$, $d_{yz}$), and three singly degenerate bands $a_1$, $a_2$, $a_3$ ($d_{xy}$, $d_{x^2-y^2}$, and $d_{z^2}$) for the $MP_4$ nanowire except for $CrP_4$. For $CrP_4$, the residual unpaired electrons can fill one of the doubly degenerate orbitals and the other is empty, resulting in five single d orbitals. In anticube configurations, five 3d orbitals of metal atoms can be split into doubly degenerate bands e1($d_{xy}$, $d_{x^2-y^2}$), e2($d_{xz}$, $d_{yz}$), and a singly degenerate band a($d_{z^2}$). Their density of states is shown in Fig. S5.† It also shows that the direction of electron transfer is from the metal

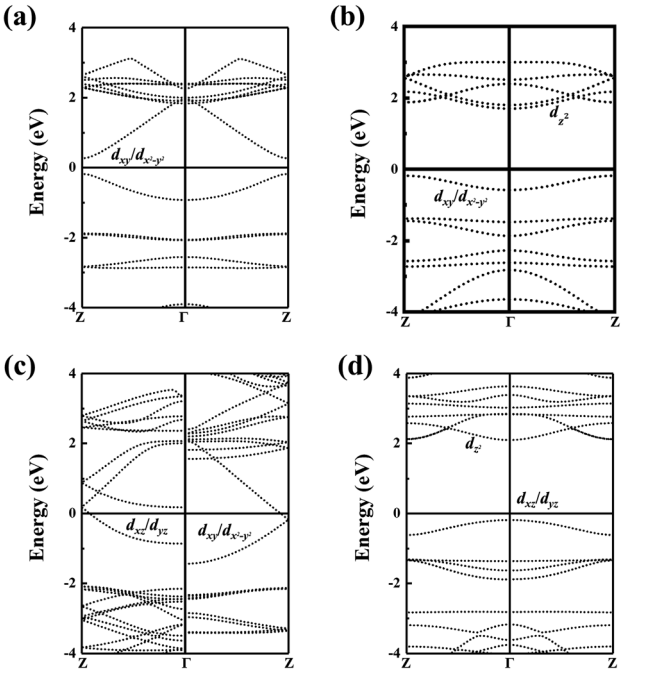


Fig. 2 The electronic band structures for (a) $ScP_4$, (b) $TiP_4$, (c) $CrP_4$, and (d) $FeP_4$ nanowires at the HSE06 level.

atom to the $P_4$ ring using the Bader charge analysis (Table 1), and residual unpaired d electrons account for the existence of magnetism.

Furthermore, we have plotted the electronic configuration of metal atoms to understand the diverse magnetic ground states in $CrP_4$ and $FeP_4$ nanowires. Based on the crystal field splitting theory and Bader charge analysis, the electronic configuration of metal ions in $CrP_4$ and $FeP_4$ nanowires are shown in Fig. S10.† As shown, both Cr and Fe ions have half-filled orbitals and the cation–anion–cation bond angle is 180°. According to the super exchange interaction theory,[45] two magnetic ions with half-occupied orbitals coupled through an intermediary nonmagnetic ion lead to a strong anti-ferromagnetic coupling, which confirmed the antiferromagnetic coupling in $FeP_4$ nanowires (Fig. S10(a)†). However, for $CrP_4$, the $P_4$ ring is slightly magnetized according to the spin charge density (Fig. S8(c)†), leading to the spin exchange pathway in Fig. S10(b)† and ferromagnetic coupling between Cr ions.

Considering the rotation of $P_4$ rings, we have also investigated the meta-stable phase of $MP_4$ nanowires and it shows that $ScP_4$ and $TiP_4$ can be stabilized in both regular quadrangular prism (Q-type) and anticube (A-type) configurations (Fig. S3†), corresponding to AFM and FM ground states, respectively, indicating a novel configuration-dependent magnetism. According to their electronic band structures (Fig. S7†), $ScP_4$ is a BMS (Bipolar Magnetic Semiconductor)[46] material of A-type and $TiP_4$ is a ferromagnetic metal of Q-type, showing a configuration tunable magnetism.

Based on the Mermin–Wagner theorem,[47] long-range magnetic order is absent for any infinitely strict one-dimensional isotropic system at non-zero temperature.

However, the relatively large magnetic crystalline anisotropic energy can help to hinder thermal fluctuation and stabilize the long-range ordering in one-dimensional or quasi-one-dimensional systems.[48] Then, non-collinear calculations are conducted and the results in Table S2† show that easy-axis of $MP_4$ (M = Sc, Ti, Cr, Fe) is normal to the nanowires and the magnetic anisotropic energy values are 0.18, 13.58, 77.86, and 326.18 μeV per atom. $TiP_4$, $CrP_4$ and $FeP_4$ are higher or comparable to the bulk b.c.c.Fe (−1.4 μeV per atom), bulk h.c.p.Co (−65 μeV per atom), bulk f.c.c.Co (1.8 μeV per atom), and bulk f.c.c.Ni (2.7 μeV per atom),[49,50] suggesting the possibility of maintaining the long-range magnetic ordering. Also, the long-range magnetic order can be stabilized by the interchain coupling of $MP_4$ nanowires. Then, we calculated the inter-chain coupling between two $CrP_4$ nanowires with an optimized distance of about 3.8 Å (Fig. S11†). It was found that the inter-chain magnetic coupling is FM, which is 0.72 meV $M^{-1}$ lower than AFM coupling in energy with a $J$ value of 0.26 meV. This value is relatively larger than that of *p*-nitrophenyl nitroxide (*p*-NPNN), which exhibits a Curie temperature of 0.65 K and the interchain coupling $J$ is estimated to be about 0.1 K (0.009 meV).[51]

## Conclusions

In summary, this work reports four types of $MP_4$ inorganic metallocene nanowires (M = Sc, Cr, Ti, Fe) that exhibit different electronic and magnetic properties. Our calculations show that $MP_4$ clusters can form stable one-dimensional nanowires. $ScP_4$, $TiP_4$ and $FeP_4$ nanowires are AFM semiconductors, while $CrP_4$ is an FM metal in the ground state. Phonon spectrum calculations and AIMD simulations demonstrate the lattice and thermodynamic stability of these nanowires. The formation of $MP_4$ nanowires *via* assembly of the $P_4$ ring and metal atoms is exothermic. Both $ScP_4$ and $TiP_4$ can be stabilized in the Q-type and A-type, corresponding to AFM and FM ground states, respectively, suggesting a novel configuration-dependent magnetism. These results reveal the potential application of $MP_4$ nanowires in spintronics. This work can promote the development of one-dimensional spintronics based on the inorganic molecular complexes.

## Author contributions

X. W. and H. L. designed the project. Y. J. and H. L. performed the calculation and analysed the data. Y. J., H. L., and X. W. wrote the manuscript.

## Conflicts of interest

There are no conflicts to declare.

## Acknowledgements

The authors gratefully acknowledge the financial support from the National Natural Science Foundation for Distinguished Young Scholars (Grant 22225301), the National Natural Science Foundation of China (Grants 22303092, 22321001), the Strategic Priority Research Program of the Chinese Academy of Sciences (Grant XDB0450101), and the support from the Super Computer Center of USTCSCC and SCCAS.

## References

1 T. J. Kealy and P. L. Pauson, *Nature*, 1951, **168**, 1039–1040.
2 S.-J. Wang, Y.-F. Wang and C. Cai, *J. Phys. Chem. C*, 2015, **119**, 16256–16262.
3 S.-J. Wang, Y. Li, D. Wu, Y.-F. Wang and Z.-R. Li, *J. Phys. Chem. A*, 2012, **116**, 9189–9196.
4 X. Liu, Y. Tan, Z. Ma and Y. Pei, *J. Phys. Chem. C*, 2016, **120**, 27980–27988.
5 N. Hosoya, R. Takegami, J.-I. Suzumura, K. Yada, K. Miyajima, M. Mitsui, M. B. Knickelbein, S. Yabushita and A. Nakajima, *J. Phys. Chem. A*, 2014, **118**, 8298–8308.
6 T. Xie and W. Qin, *J. Phys. Chem. C*, 2016, **120**, 24498–24502.
7 L. Münzfeld, S. Gillhuber, A. Hauser, S. Lebedkin, P. Hädinger, N. D. Knöfel, C. Zovko, M. T. Gamer, F. Weigend, M. M. Kappes and P. W. Roesky, *Nature*, 2023, **620**, 92–96.
8 J. L. Wang, X. Y. Zhang, P. V. R. Schleyer and Z. F. Chen, *J. Chem. Phys.*, 2008, **128**, 104706.
9 Y. X. Wang, C. C. Sun, Z. D. Yang, H. Yu, P. Pan, L. Pei, G. L. Zhang and Y. Y. Hu, *Chem. Phys.*, 2019, **523**, 1–6.
10 X. Liu, Y. Tan, G. Zhang and Y. Pei, *J. Phys. Chem. C*, 2018, **122**, 16168–16177.
11 Z. Yang, B. L. Zhang, X. G. Liu, Y. Z. Yang, X. Y. Li, S. J. Xiong and B. S. Xu, *Org. Electron.*, 2013, **14**, 2916–2924.
12 P. Gain, R. Jana and A. Datta, *J. Phys. Chem. A*, 2021, **125**, 3362–3368.
13 L. Zhou, S.-W. Yang, M.-F. Ng, M. B. Sullivan, V. B. C. Tan and L. Shen, *J. Am. Chem. Soc.*, 2008, **130**, 4023–4027.
14 L. Wang, X. Gao, X. Yan, J. Zhou, Z. Gao, S. Nagase, S. Sanvito, Y. Maeda, T. Akasaka, W. N. Mei and J. Lu, *J. Phys. Chem. C*, 2010, **114**, 21893–21899.
15 X. Li, H. Lv, J. Dai, L. Ma, X. C. Zeng, X. Wu and J. Yang, *J. Am. Chem. Soc.*, 2017, **139**, 6290–6293.
16 K. Miyajima, A. Nakajima, S. Yabushita, M. B. Knickelbein and K. Kaya, *J. Am. Chem. Soc.*, 2004, **126**, 13202–13203.
17 J. Wang, P. H. Acioli and J. Jellinek, *J. Am. Chem. Soc.*, 2005, **127**, 2812–2813.
18 H. Xiang, J. Yang, J. G. Hou and Q. Zhu, *J. Am. Chem. Soc.*, 2006, **128**, 2310–2314.
19 L. Wang, Z. Cai, J. Wang, J. Lu, G. Luo, L. Lai, J. Zhou, R. Qin, Z. Gao, D. Yu, G. Li, W. N. Mei and S. Sanvito, *Nano Lett.*, 2008, **8**, 3640–3644.
20 X. Wu and X. C. Zeng, *J. Am. Chem. Soc.*, 2009, **131**, 14246–14248.
21 Z. Zhang, X. Wu, W. Guo and X. C. Zeng, *J. Am. Chem. Soc.*, 2010, **132**, 10215–10217.
22 X. Zhang, J. Han, Y. Liu and J. Wang, *J. Phys. Chem. C*, 2012, **116**, 5414–5419.
23 Y. Li, Z. Zhou and Z. Chen, *J. Phys. Chem. A*, 2012, **116**, 1648–1654.

24 X. Zhang, M.-F. Ng, Y. Wang, J. Wang and S.-W. Yang, *ACS Nano*, 2009, **3**, 2515–2522.
25 M. Wu, J. D. Burton, E. Y. Tsymbal, X. C. Zeng and P. Jena, *J. Am. Chem. Soc.*, 2012, **134**, 14423–14429.
26 N. Kuhn, E.-M. Horn, R. Boese and N. Augart, *Angew Chem. Int. Ed. Engl.*, 1988, **27**, 1368–1369.
27 G. Frenking, K. Wichmann, N. Fröhlich, C. Loschen, M. Lein, J. Frunzke and V. M. Rayón, *Coord. Chem. Rev.*, 2003, **238**, 55–82.
28 E. Urnezius, W. W. Brennessel, C. J. Cramer, J. E. Ellis and P. V. Schleyer, *Science*, 2002, **295**, 832–834.
29 J. Trygg, B. Johansson, O. Eriksson and J. M. Wills, *Phys. Rev. Lett.*, 1995, **75**, 2871–2874.
30 Z.-C. Wang, L. Qiao, Z.-M. Sun and M. Scheer, *J. Am. Chem. Soc.*, 2022, **144**, 6698–6702.
31 G. Kresse and J. Furthmuller, *Phys. Rev. B: Condens. Matter Mater. Phys.*, 1996, **54**, 11169–11186.
32 G. Kresse and J. Furthmuller, *Comput. Mater. Sci.*, 1996, **6**, 15–50.
33 J. P. Perdew, K. Burke and M. Ernzerhof, *Phys. Rev. Lett.*, 1996, **77**, 3865–3868.
34 P. E. Blöchl, *Phys. Rev. B: Condens. Matter Mater. Phys.*, 1994, **50**, 17953–17979.
35 G. Kresse and D. Joubert, *Phys. Rev. B: Condens. Matter Mater. Phys.*, 1999, **59**, 1758–1775.
36 Y. G. Zhang, Z. Cui, B. S. Sa, N. H. Miao, J. Zhou and Z. M. Sun, *Nanoscale Horiz.*, 2022, **7**, 276–287.
37 S. Y. Wang, N. X. Miao, K. H. Su, V. A. Blatov and J. J. Wang, *Nanoscale*, 2021, **13**, 8254–8263.
38 J. Heyd, G. E. Scuseria and M. Ernzerhof, *J. Chem. Phys.*, 2006, **124**, 219906.
39 S. Grimme, *J. Comput. Chem.*, 2006, **27**, 1787–1799.
40 A. Togo and I. Tanaka, *Scr. Mater.*, 2015, **108**, 1–5.
41 K. Momma and F. Izumi, *J. Appl. Crystallogr.*, 2011, **44**, 1272–1276.
42 V. Wang, N. Xu, J. C. Liu, G. Tang and W. T. Geng, *Comput. Phys. Commun.*, 2021, **267**, 108033.
43 P. Chen, N. Li, X. Chen, W.-J. Ong and X. Zhao, *2D Mater.*, 2017, **5**, 014002.
44 L. Shen, S. W. Yang, M. F. Ng, V. Ligatchev, L. P. Zhou and Y. P. Feng, *J. Am. Chem. Soc.*, 2008, **130**, 13956–13960.
45 J. B. Goodenough, *Magnetism and the Chemical Bond*, Wiley-Interscience, New-York, 1963.
46 H. D. Wang, Q. Q. Feng, X. X. Li and J. L. Yang, *Research*, 2022, 9857631.
47 N. D. Mermin and H. Wagner, *Phys. Rev. Lett.*, 1966, **17**, 1133–1136.
48 P. Gambardella, A. Dallmeyer, K. Maiti, M. C. Malagoli, W. Eberhardt, K. Kern and C. Carbone, *Nature*, 2002, **416**, 301–304.
49 A. N. Anisimov, M. Farle, P. Poulopoulos, W. Platow, K. Baberschke, P. Isberg, R. Wäppling, A. M. N. Niklasson and O. Eriksson, *Phys. Rev. Lett.*, 1999, **82**, 2390–2393.
50 J. Trygg, B. Johansson, O. Eriksson and J. M. Wills, *Phys. Rev. Lett.*, 1995, **75**, 2871–2874.
51 M. Takahashi, P. Turek, Y. Nakazawa, M. Tamura, K. Nozawa, D. Shiomi, M. Ishikawa and M. Kinoshita, *Phys. Rev. Lett.*, 1991, **67**, 746–748.